FLOW CONTROL ON A TWO-DIMENSIONAL CIRCULAR CYLINDER

Michael Amitay, Andrew M. Honohan, and **Ari Glezer**
School of Mechanical Engineering
Georgia Institute of Technology
Atlanta, GA 30332-0405, USA

ABSTRACT

Controlled modification of the global performance of aerodynamic surfaces is achieved by fluidic manipulation of their apparent aerodynamic shape and is effected by the interactions of arrays of synthetic jet actuators with the cross flow within a finite streamwise domain that displaces the local streamlines near the surface and thereby induces an 'apparent' modification of the flow boundary and of the streamwise pressure gradient. The operating frequency of the control jets is high enough so that the actuation period is at least an order of magnitude *lower* than the relevant characteristic time scale of the flow. Therefore, the finite interaction domains between the control jets and the cross flow are quasi-steady and hence the induced aerodynamic forces are virtually time-invariant. Earlier work at Georgia Tech demonstrated the utility of this control approach for the suppression of flow separation at post-stall angles of attack. The present work focuses on the modification of the aerodynamic characteristics of a circular cylinder at subcritical Reynolds number where the localized displacement of the streamlines over the boundary is achieved using jet actuators and miniature [$O(0.01D)$] surface-mounted passive obstruction.

INTRODUCTION

Flow control strategies for external aerodynamic surfaces have mostly focused on mitigation of flow separation which can be precipitated by an adverse pressure gradient (e.g., on a lifting surface) or by a sharp discontinuity in the flow boundary (e.g., a cavity or a bluff trailing edge). Control has been typically achieved by exploiting the combined narrow-band receptivity of the separating shear layer and the upstream boundary layer to relatively low-level external actuation (e.g., Ho and Huerre, 1984) which therefore can only be applied within a limited spatial domain ahead of separation. This approach to flow control has been applied with varying degrees of success since the early 1980s to restore aerodynamic performance of stalled airfoils and flaps (e.g., Ahuja and Burrin 1984, Neuburger and Wygnanski 1987, and Seifert et al. 1993) in which the actuation period nominally scales with the advection time over the length of the affected flow domain downstream of separation. It is noteworthy that the time-periodic transport and shedding of vorticity concentrations along the lifting surface and into its wake, respectively are accompanied by time-periodic variations of surface pressure distribution and of the global aerodynamic forces (Amitay and Glezer, 1999 and 2002).

A radically different approach to the control of flow separation on lifting surfaces emphasizes fluidic modification of the "apparent" aerodynamic shape of the surface upstream of separation with the objective of altering the streamwise pressure gradient to achieve complete or partial bypass (or suppression) of separation. Actuation is effected by forming a controlled interaction domain between a surface-mounted fluidic actuator (e.g., a synthetic jet) and the cross flow above the surface. As demonstrated by Honohan et al. (2000), the interaction domain between a high-frequency synthetic jet and the cross flow over the surface of a two-dimensional cylinder displaces the local streamlines of the cross flow and thereby induce a 'virtual' change in the shape of the surface (measuring roughly 2-4 actuation wavelengths). The resulting change in the streamwise pressure gradient alters the evolution of the boundary layer and leads to a delay in separation. In contrast to control approaches that rely on global manipulation of the instability of the separating shear layer and are based on a characteristic actuation period that scales with the advection time of the affected flow domain "virtual" surface shaping is based on actuation having a characteristic wavelength that is at least an order of magnitude smaller than the relevant local or global length scale in the flow. In fact, "virtual" surface shaping emphasizes an actuation frequency that is high enough so that the interaction between the actuator and the cross flow upstream of separation is essentially time-invariant on the global time scale of the flow and therefore global effects (e.g., vorticity shedding) are effectively *decoupled* from the actuation frequency. This approach has been successfully applied to modify or control the evolution of both wall bounded and free shear flows (e.g., stalled airfoils, Amitay et al., 1997, and jet vectoring, Smith and Glezer, 2002, respectively).

Although the interest in control of separation for aerodynamic applications has been primarily focused on 2-D and 3-D airfoils, some control strategies have been investigated in the nominally two-dimensional flow around circular cylinders (e.g., Williams et al., 1991 and Pal & Sinha, 1997). This simple geometry is particularly attractive it minimizes higher-order effects of a *specific* global (e.g.,

airfoil) geometry and has the distinct advantage that the baseline flow is extensively documented including the evolution with Reynolds number of flow separation (e.g., Roshko and Fiszdon, 1969). In the earlier experiments of Amitay et al. (1997 and 1998), the lift and drag forces on a circular cylinder were significantly altered by the formation of small quasi steady closed recirculating flow regimes near the surface over a range of azimuthal locations between the front and rear stagnation points using synthetic (i.e., zero mass flux) jet actuators (Smith and Glezer, 1997). Similar to the effects of fluidic actuation, it is well known that the flow around bluff bodies at sub-critical Reynolds numbers can be significantly modified by placing small physical obstructions upstream from the location of boundary layer separation. Prandtl demonstrated that the use of a small diameter wire mounted azimuthally around the surface of a sphere delays boundary layer separation (Prandtl et al., 1914). Such a device, commonly referred to as a "trip", is frequently thought to induce premature transition to turbulence within the boundary layer, and consequently delay separation presumably owing to enhanced momentum transfer with the (outer) cross flow (e.g., Fage & Warsap, 1929, James & Truong, 1972, Igarashi, 1986 and Hover, Tvedt & Triantafyllou, 2001). In fact, placement of a trip wire on the surface of a circular cylinder can lead to reduction in drag and can even generate lift when positioned asymmetrically (James & Troung, 1972). These observations are useful in formulating an alternative explanation of the physical mechanism by which trip wires alter bluff body aerodynamics. As shown in the present paper, the placement of a wall-mounted obstruction upstream from separation brings about a change in the cylinder's apparent aerodynamic shape due to the formation of a local separation bubble, that apparently has a similar effect to that of bubbles that appear upstream of separation during the natural occurrence of the drag crisis at critical Reynolds numbers (Achenbach, 1968). As in the case of fluidic actuation, the streamwise pressure gradient is altered by the local change in curvature of the flow, leading to changes in boundary layer evolution, and the location of separation

The present paper describes the modifications of the aerodynamic characteristics of a circular cylinder at sub-critical Reynolds numbers. These modifications are induced by asymmetric displacement of the cross flow streamlines near the flow boundary which is achieved by the interaction of the cross flow with a surface mounted synthetic jet actuator and by a miniature, surface mounted passive obstruction. Furthermore, the effects of the location and size of the obstruction is also presented.

EXPERIMENTAL SETUP

The bulk of the experiments that are described in the present paper are conducted in two wind tunnel set ups. Aerodynamic measurements were conducted in an open-return low-speed wind tunnel having a square test section measuring 0.91 m on the side (maximum speed 50 m/sec and turbulence level less than 0.15%). High-resolution particle image velocimetry (PIV) along the surface of the cylinder was accomplished in a close-return wind tunnel having a test section which is essentially a 2-D slice (5 cm wide) of the test section in the open return wind tunnel. The cylinder model that was used in the present experiments is a 63.2 mm diameter circular cylinder that can be rotated about its spanwise axis, has a pair of adjacent spanwise jet actuators (2.5 mm apart, each 0.5 mm wide) and an azimuthal array of 47 equally-spaced pressure ports. High-frequency actuation jets are generated using piezoelectric drivers in compact, shallow cavities underneath the surface of the cylinder (Amitay et al., 1997 and Honohan et al., 2000). As noted in the introduction, passive aerosurface modification is also provided by a surface-mounted cylindrical obstruction having a circular cross section (diameter d) that is collinear with the longitudinal axis of the primary cylinder and is mounted along its center (actuated) segment. The azimuthal positions of the jet and the obstruction relative to the upstream stagnation point are referenced by the angle γ. Time-averaged surface pressure distributions are obtained using a differential pressure transducer. Distributions of the streamwise and cross-stream velocity components in the near wake of the airfoil and the cylinder are measured using a miniature x-wire probe mounted on a computer-controlled traversing mechanism. The nominally two-dimensional flow field around the cylinder is measured using a commercial PIV system. A 1008 x 1016 CCD camera is used to capture high resolution images (8.88 μm/pixel, yielding a spatial resolution of 0.133 mm) over an extended domain along the surface of the cylinder by acquiring nine to twelve sets of overlapping images.

FLOW CONTROL ON A CIRCULAR CYLINDER

An example of the global effects of jet actuation on the

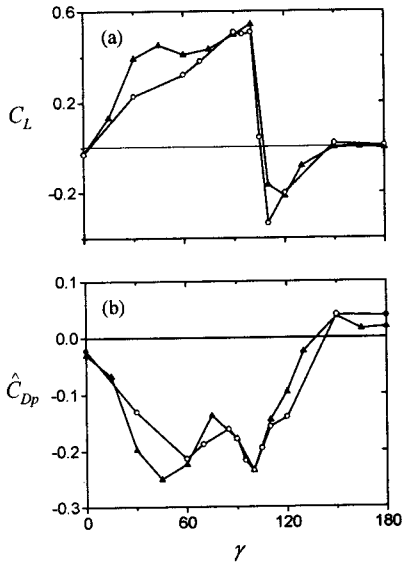

Figure 1. Variation of (a) C_L and (b) $\hat{C}_D$ with jet angle. $St_D = 2.5$ (○) and 4.5 (▲), $Re_D = 75{,}500$.

global aerodynamic characteristic of the circular cylinder is presented in Figures 1a and b which shows the variation of lift and (pressure) drag, respectively with the azimuthal position of the actuation jet γ in a series of wind tunnel experiments at $Re_D = 75{,}500$. The lift coefficient C_L and of the normalized increment in (pressure) drag $\hat{C}_D$ (where $\hat{C}_D = C_{Dactuated} / C_{Dbaseline} - 1$) are computed from

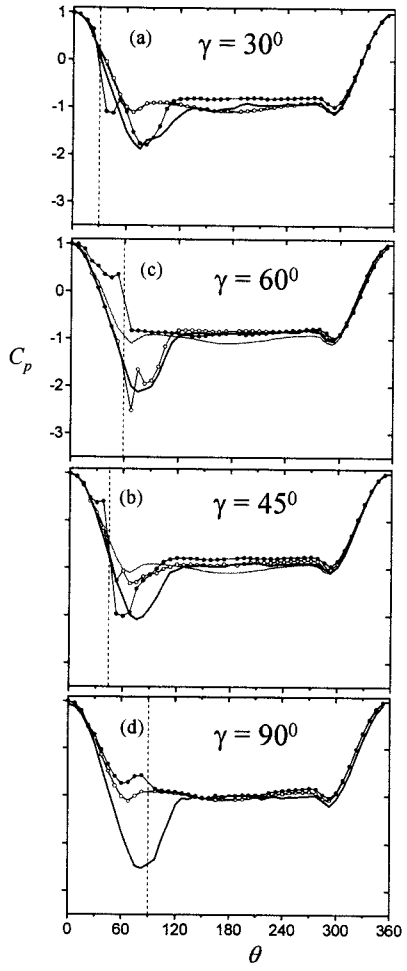

Figure 2. $C_p(\theta)$: $d/D = 0.0082$ (○), 0.041 (●); baseline (—), jet actuation (—).

measurements of azimuthal distributions of the cylinder surface pressure coefficient $C_p(\theta)$ at each jet position in the absence (baseline) and presence of actuation. These measurements are obtained at two actuation frequencies 740 Hz ($St = 2.5$) and 1300 Hz ($St = 4.5$) where, for reference, the "natural" shedding frequency is $St_s = 0.21$. As is evident from these data, the distributions of C_L and $\hat{C}_D$ are qualitatively independent of the actuation frequency and while $\hat{C}_D$ decreases with γ (i.e., a decrease in pressure drag) by up to approximately 25%, C_L increases with γ with a maximum value of approximately 0.54 at $\gamma = 100°$. It is remarkable that the lift force reverses its direction at $\gamma > 100°$ while $\hat{C}_D$ begins to increase (i.e., an increase in the drag force). The lift force vanishes at $\gamma = 135°$ at both actuation frequencies, and the largest reversed lift force is –0.27. As shown in the earlier work of Honohan et al. (2000), and by the pressure data the reduction in drag within the range $60° < \gamma < 110°$ is associated with an extended region of attached flow on the top surface of the cylinder as a result of a streamwise domain of a favorable pressure gradient that is induced along the surface of the cylinder owing to the displacement of the cross flow by the interaction domain.

The main focus of the present paper is to explore the concept of localized flow displacement and its effect on the evolution of the streamwise pressure distribution and consequently on flow separation and the global aerodynamic forces. To this end, the effects induced by the interaction domain between the jet and the cross flow are compared to the displacement of the outer flow by a miniature obstruction having a circular cross section that is mounted on the surface of the cylinder at the same azimuthal positions of the jet. To begin with, distributions of the variation of the azimuthal pressure coefficient $C_p(\theta)$ for two characteristic obstructions ($d/D = 0.0082$ and 0.041) placed at several positions γ are shown in Figures 2a-d along with corresponding pressure distributions for the baseline flow (i.e., in the absence of actuation) and in the presence of a jet actuation ($C_\mu = 7 \cdot 10^{-4}$, $f_{act} = 740$ and $St_D = 2.5$). At $\gamma = 30^0$ (which is where traditionally "tripping" devices are placed on cylinders at sub-critical Reynolds numbers to achieve "supercritical"-like pressure distributions), the smaller obstruction ($d/D = 0.0082$) has minimal effect of the pressure distribution. However, an obstruction having a larger characteristic dimension ($d/D = 0.04$) results in a significant alteration of the pressure distribution. The pressure distribution shows a slight increase in the pressure upstream of the obstruction due to blockage and the presence of a closed separation bubble immediately downstream of the obstruction as is evidenced by the local decrease of the pressure coefficient relative to the baseline flow (i.e., a favorable pressure gradient) which is followed by a local minimum and recovery and attachment at $\theta \approx 60°$ (see also Figure 4b). It is remarkable that this local minimum is then followed by a second local minimum (suction peak) at $\theta \approx 90°$ and ultimately by separation at $\theta \approx 120°$. The second pressure minimum is presumably associated with acceleration of the outer flow, which results in the delay of the separation and is also accompanied by an increase in the cylinder's base pressure which contributes to the reduction in pressure drag (see also Figure 3b). By comparison, the pressure distribution that is induced by the jet actuation is similar in general trends, but does not show pressure changes due to the presence of the interaction domain (ostensibly because they are below the resolution of the pressure taps and because the magnitude of the local changes is rather small). While the suction peak in the presence of the jet is similar in magnitude to the peak that is induced by the obstruction, the jet induced peak is wider and separation seems to occur farther downstream ($\theta \approx 115°$ compared to $\approx 130°$ with the obstruction). Furthermore, jet actuation results in a smaller increase in the cylinder base pressure.

When $\gamma = 45^0$ (Figure 2b), both obstructions lead to the formation of a measurable separation bubble as is evident by the local decrease in pressure downstream of the obstruction. However, while the small obstruction ($d/D = 0.0082$) exhibits a two pressure peaks (as in Figure 2a for $d/D = 0.041$), the large obstruction ($d/D = 0.041$) results in a single pressure peak that is similar to the pressure distribution that is induced by the jet but (with equal magnitude peak) but is somewhat narrower and indicates that separation occurs upstream compared to jet actuation ($\theta \approx 115°$ compared to 125°). Also, the effect of the blockage in the presence of the large obstruction is rather significant and certainly contributes to drag (although the increase in base pressure is still substantial and larger than in the presence of the jet). At at $\gamma = 60^0$ (Figure 2c), the larger obstruction ($d/D = 0.041$) leads to complete flow separation

immediately downstream of the obstruction ($\theta \approx 65°$) and substantial blockage effect upstream (where the base pressure is the same as in the baseline in the absence of actuation). However, the performance of the smaller obstruction ($d/D = 0.0082$), is remarkably different. With the exception of a local suction peak on the top surface of the cylinder ($C_p \approx -2.5$) the overall pressure distribution is quite similar to the distribution that is induced by the presence of the jet. Separation appears to occur at $\theta \approx 110^0$, and the base pressure slightly exceeds the base pressure in the presence of jet actuation.

These effects clearly indicate that the modified flow about the cylinder is extremely sensitive to the combination of the characteristic dimension of the obstruction and its azimuthal position. While the former affects the characteristic size of the induced separated flow domain, the latter affects the magnitudes of the favorable and adverse pressure gradients that are induced by the presence of the obstruction and also the effect of the upstream flow blockage (note that owing to suction that is induced by the jet its blockage effects are rather minimal).

Perhaps the most striking difference between actuation with the jet and the obstruction is demonstrated when these devices are placed just *downstream* of separation in the baseline flow ($\gamma = 90°$, Figure 2d). While jet actuation leads to a further increase in the suction peak the obstruction (at least within the range tested here) has virtually no significant effect. When $\gamma = 110°$ (not shown), jet actuation continues to affect the global flow on the top and bottom surfaces (resulting in an approximately zero lift force as a precursor to the reversal in lift force). However, neither obstruction has any effect on the pressure distribution.

The sensitivity of the global aerodynamic forces to the characteristic obstruction size d/D is shown in Figures 3a (C_L) and b ($\hat{C}_D$) for several locations of the obstruction. When $\gamma = 30°$, C_L and $\hat{C}_D$ increase and decrease, respectively, but these changes appear to saturate for $d/D > 0.035$ (which is similar to the effect of synthetic jet actuation as shown by Amitay et al., 1997). However, as γ

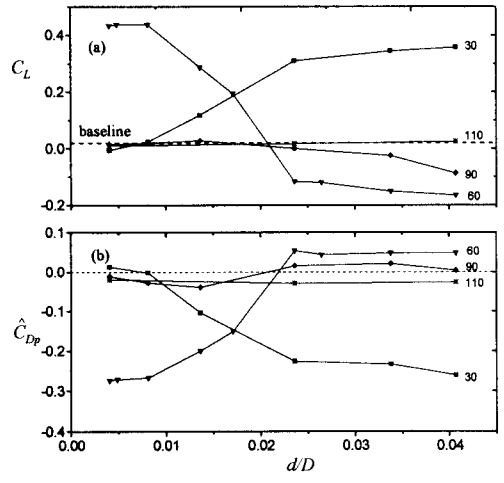

Figure 3. Variations of (a) C_L and (b) $\hat{C}_D$ with d/D.

increases the trends in C_L and $\hat{C}_D$ are substantially reversed. For $\gamma = 60°$, C_L and $\hat{C}_D$ are largest and smallest, respectively, for $d/D < 0.01$ however, an additional increase in d/D results in substantial degradation of the aerodynamic forces (i.e., a decrease in C_L and an increase in drag) C_L becomes negative and $\hat{C}_D$ becomes positive for $d/D > \sim 0.2$. As noted in connection with Figures 2d and e, when $\gamma \geq 90^0$ (i.e., downstream of the separation for the baseline flow) placing an obstruction on the surface has very small effect on C_L and $\hat{C}_D$ (the change in $\hat{C}_D$ is less than 3%, which is within the measurement error).

Details of the interaction between the actuation (by the jet and an obstruction) and the cross flow on the top surface of the cylinder can be compared with the baseline flow using maps of spanwise vorticity concentrations that are obtained from PIV measurements (Figures 4a-c). The measurements are taken at $Re_D = 75{,}000$ and the obstruction is selected so that the lift and drag forces for $d/D = 0.014$ are within 2 % of the forces that are effected by a synthetic jet at $St_D = 4.0$, $C_\mu = 1.0 \cdot 10^{-3}$ (i.e., $C_L = 0.50$, $C_D = 0.87$ for synthetic jet actuation and $C_L = 0.49$ and $C_D = 0.86$ for the obstruction). The baseline flow (Figure 4a) separates at $\theta \approx 95°$ and the separated flow domain is marked by the presence of negative (i.e., CCW) vorticity near the surface. When the obstruction is placed on the surface ($\gamma = 60°$, Figure 4b), the flow separates locally and reattaches at $\theta \approx 75°$ (i.e., $-0.25 \leq x/D \leq -0.12$) although the boundary layer downstream of the attachment region is considerably thicker than for the baseline flow at the same azimuthal domain. Separation occurs at $\theta \approx 120°$ and the streamwise spreading rate of the separated shear layer appears to be smaller than for the unforced flow presumably owing to increased speed and turning of the outer flow. The vorticity maps even capture the blockage effects and thickening of the boundary layer upstream of the obstruction. Finally, the effects of jet actuation are shown in Figure 4c. It is remarkable that even though both the jet and the obstruction yield similar aerodynamic forces and lead to flow attachment the most prominent difference between the vorticity maps is that the flow displacement by the obstruction is substantially larger than the displacement by the interaction domain of the jet. Furthermore, the boundary layer downstream of the jet interaction domain is substantially thinner than the corresponding boundary layer downstream of the obstruction.

As noted in the introduction, it has long been the notion that the placement of "trip" wires on the surface of two-dimensional cylinders at sub-critical Reynolds numbers results in pressure distributions that are similar to the distributions at higher Reynolds numbers when the flow on the cylinder is presumably turbulent. Therefore, it is of interest to compare distributions of the Reynolds stresses for the three flow configurations as shown in Figures 5a-i [baseline (a-c), obstruction (d-f) and jet actuation (g-i)]. For each case, three maps of the time-averaged stresses include (from top to bottom) $\overline{u_r' u_r'}$, $\overline{u_\theta' u_\theta'}$, and $\overline{u_r' u_\theta'}$. The separating boundary layer and the ensuing shear layer are easily identified from concentrations of $\overline{u_\theta' u_\theta'}$ and $\overline{u_r' u_\theta'}$ (Figures 5b, and c). The most striking feature in the Reynolds stresses maps of both the obstruction and the actuated flows is the diminution in the magnitude of the Reynolds stresses in the shear layer compared to the baseline flow. As in the vorticity maps in Figure 4b the separation bubble that is formed by the obstruction is clearly resolved by concentrations of Reynolds stresses (which is not the case for actuation by the jet). It might be argued (and

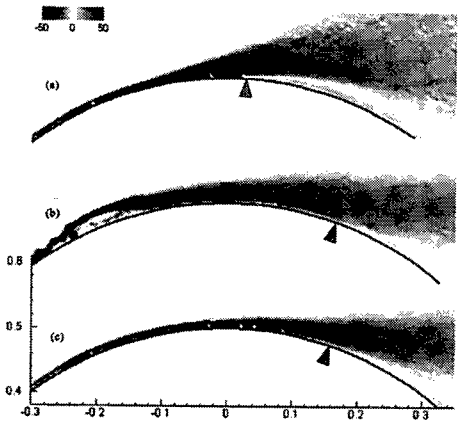

Figure 4. Spanwise vorticity distributions: (a) baseline, (b) obstruction at $\gamma = 60°$ and (c) jet actuation at $\gamma = 60°$.

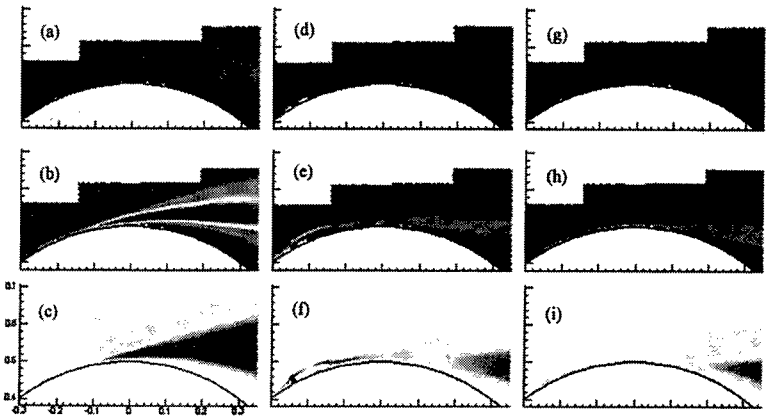

Figure 5. Distributions of the Reynolds stresses for baseline (a-c), obstruction (d-f) and jet actuation (g-i)].

experimental evidence supports that Amitay et al. (2001) that similar to the jet, the interaction of the obstruction with the cross flow and the extended flow attachment leads to partial suppression of vortex shedding from the cylinder and therefore to a reduction in the Reynolds stresses that typically also account for "potential" velocity fluctuations. Nevertheless, the reduction in the Reynolds stresses within the separating shear layer owing to the presence of both the obstruction and the synthetic jet is an indication that the delay in separation is not merely the result of turbulent transition within the surface boundary layer. Therefore, it may be argued that the presence of the separation bubble, which modifies the apparent aerodynamic shape of the cylinder, is ultimately responsible for the changes in the aerodynamic forces.

The modification of the aerodynamic forces on the cylinder is accompanied by substantial changes in the structure of its wake which are studied using hot wire anemometry. Cross stream distributions of time-averaged streamwise and cross stream velocity components and of the corresponding normalized distributions of the rms velocity fluctuations u' and v' are shown in Figures 6a-d, respectively (the distributions of the baseline flow are plotted using solid lines). For the baseline flow, the cross stream distributions of the mean and as well as of the fluctuating velocity components are reasonably symmetric about the cylinder's centerline ($y/D = 0$), indicating that the lift coefficient is nearly zero. As can be seen in Figure 6a, the establishment of net lift force on the cylinder and the reduction in its drag owing to the obstruction or the jet actuator are accompanied by a downward displacement of the wake (opposite to the direction of the lift force) and a smaller velocity deficit. While the effects of the obstruction and the jet are very similar, it appears that the velocity deficit in the presence of the obstruction is somewhat smaller than with the jet. Furthermore, the cross stream velocity in the forced flow exhibits an offset which corresponds to downwash motion of the flow. As expected, based on concentrations of Reynolds stresses in Figure 6, the forcing also results in lower levels of rms velocity fluctuations (Figure 6c). Finally, as noted in connection with Figure 5, earlier work at Georgia Tech has indicated that the formation of the interaction domain between the actuation (i.e., jet or obstruction) and the cross flow and the attachment of the separated flow to the cylinder surface is accompanied by substantial weakening of the instability that leads to the shedding of regular vorticity concentrations into the wake of the cylinder. This is confirmed by considering cross stream distributions of the time-averaged vorticity (Figure 6d) which interestingly enough exhibits only a slight asymmetry about the wake center and shows that compared to the baseline flow, the vorticity magnitude is smaller across the entire wake.

CONCLUSIONS

The global performance of aerodynamic surfaces can be modified by manipulation of their apparent aerodynamic shape using fluidic based actuation (Amitay at al., 1997). This is achieved by the formation of a quasi steady finite streamwise domain that is formed by the interaction between arrays of synthetic jet actuators and the cross flow and displaces the local streamlines near the surface and thereby induces an 'apparent' modification of the flow boundary and of the streamwise pressure gradient.

The present work focuses on the modification of the aerodynamic characteristics of a circular cylinder at subcritical Reynolds number where the localized flow displacement over the boundary is achieved using both a jet actuators and a miniature [O(0.01D)] surface-mounted passive obstruction.

The experiments are conducted at a cylinder Reynolds numbers of 75,000. The interaction between the jet and the cross flow leads to substantial changes in the lift and (pressure) drag that vary with the azimuthal position of the jet γ. When $\gamma < 90°$, there is a substantial increase in lift and reduction in drag. However when the jet is placed (nominally) downstream of separation, the induced lift force on the cylinder is reversed. The present work has demonstrated that the placement of a passive obstruction ($d/D < 0.04$) can also result in substantial changes in the aerodynamic forces of the cylinder. However, these changes are very sensitive to the characteristic dimension of the obstruction and to its azimuthal position. When the

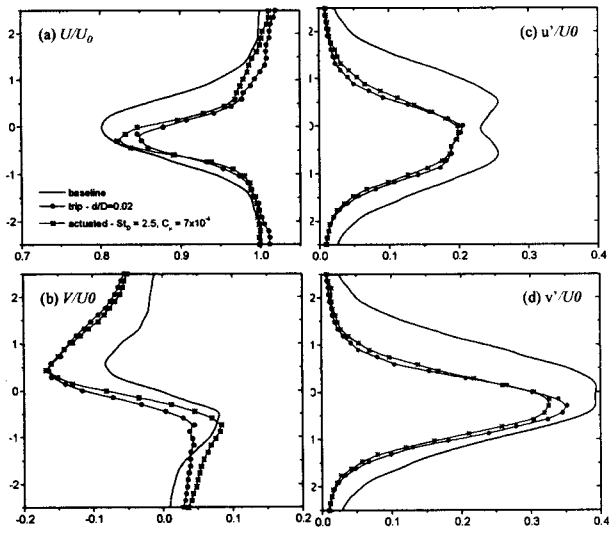

Figure 6. U/U_0, (a) V/U_0 (b), u'/U_0 (c), and v'/U_0 (d) ($x/D = 3.5$).

obstruction is placed at $\gamma = 30°$ the magnitude of the aerodynamic forces can be monotonically varied within some range of obstruction sizes ($0.01 < d/D < 0.03$). However, at $\gamma = 60°$, a relatively small obstruction ($d/D < 0.01$) can result in substantial increase in lift (0.45) and reduction in drag (27%), but a further increase in d/D leads to a rapid deterioration of its effect and even to degradation in the baseline characteristics. For $\gamma > 90°$, the effects of the obstruction vanishes completely. In fact, the most striking difference between actuation with the jet and the obstruction is demonstrated when these devices are placed just *downstream* of separation in the baseline flow. While jet actuation leads to a further changes in the aerodynamic forces (and in fact to reversal of the lift force), the obstruction (at least within the range tested here) has virtually no significant effect.

One of the important findings of the present work stems from detailed comparison of the interaction domains of the cross flow with the obstruction and the jet for which the characteristic dimension of the obstruction is selected so that the aerodynamic forces are matched to the forces that are effected by the jet. Cross stream PIV measurements near the surface of the cylinder reveal that as postulated by surface pressure measurements, the obstruction forms a close recirculating flow domain that induces similar effects to those of a jet in terms of the displacement of the cross flow and the alteration of the streamwise pressure gradient. However, for the same aerodynamic forces and similar flow attachment relative to the baseline flow, the characteristic streamwise and cross stream protrusions of the recirculating bubble that is induced by the obstruction are much larger (about an order of magnitude) than the interaction domain with the jet. Furthermore, the boundary layer downstream of the jet interaction domain is substantially thinner than the corresponding boundary layer downstream of the obstruction. Reynolds stresses maps in the presence of both the obstruction and the jet show substantial diminution in the magnitude of the Reynolds stresses in the separating shear layer compared to the baseline flow. While it might be presumed that similar to the jet, the interaction of the obstruction with the cross flow and the extended flow attachment leads to partial suppression of vortex shedding from the cylinder and therefore to a reduction in the Reynolds stresses, the reduction in the Reynolds stresses within the separating shear layer owing to the presence of both the obstruction and the synthetic jet is an indication that the delay in separation is not merely the result of turbulent transition within the surface boundary layer. Therefore, it may be argued that the presence of the separation bubble, which modifies the apparent aerodynamic shape of the cylinder, is ultimately responsible for the changes in the aerodynamic forces.

ACKNOWLEDGEMENT

This work has been supported by AFOSR, and a NASA Langley GSRP Grant to Mr. A. Honohan.

REFERENCES

Amitay M., Honohan, A., Trautman M. and Glezer A., 1997, "Modification of the Aerodynamic Characteristics of Bluff Bodies Using Fluidic Actuators", AIAA Paper 97-2004.

Amitay, M., Smith, B.L., and Glezer, A., 1998, "Aerodynamic Flow Control Using Synthetic Jet Technology", AIAA Paper 98-0208.

Fage A., & Warsap J.H., "The effects of turbulence and surface roughness on the drag of a circular cylinder," Aero. Res. Comm. R & M No. 1283, 1929.

Hover F.S., Tvedt H., & Triantafyllou M.S., "Vortex-induced vibrations of a cylinder with tripping wires," J. Fluid Mech., v448, pp. 175-195, 2001.

Huang L.S., Maestrello L. and Bryant T.D., 1987, "Separation Control Over an Airfoil at High Angles of Attack by Sound Emanating from the Surface", AIAA Paper 87-1261.

Igarashi T., "Effect of tripping wires on the flow around a circular cylinder normal to an airstream," Bull. JSME, v29, No. 255, 1986.

James D.F., and Truong Q-S, "Wind load on cylinder with spanwise protrusion," Proceedings of the ASCE, Journal of the Engineering Mechanics Division, v98, pp. 1573-1589, 1972.

Pal D. and Sinha K., 1997, "Controlling an Unsteady Separating Boundary Layer on a Cylinder with an active Compliant Wall", AIAA Paper 97-0212.

Prandtl, L.: Der Luftwiderstand von Kugeln, Nachr. Ges. Wiss. Gottingen, Math. Phys. Klasse, 1914 pp 177-190.

Roshko A. and Fiszdon W., 1969, "On the Persistence of Transition in the Near Wake". Problems of Hydrodynamics and Continuum Mechanics. Soc. Industrial and Appl. Math., Philadelphia, pp. 606-616.

Smith B. L. and Glezer A., 1997, "Vectoring and Small-Scale Motions Effected in Free Shear Flows Using Synthetic Jet Actuators", AIAA Paper 97-0213.

Williams, Acharya, Bernhardt & Yang, 1991, "The Mechanism of Flow Control on a Cylinder with the Unsteady Bleed Technique", AIAA Paper, 29th Aerospace Sciences meeting.